



Journal of Applied Research and  
Technology

ISSN: 1665-6423

[jart@aleph.cinstrum.unam.mx](mailto:jart@aleph.cinstrum.unam.mx)

Centro de Ciencias Aplicadas y  
Desarrollo Tecnológico  
México

Macías-Martínez, B.I.; Cortés-Hernández, D.A.; Zugasti-Cruz, A.; Cruz-Ortíz, B.R.;  
Múzquiz-Ramos, E.M.

Heating ability and hemolysis test of magnetite nanoparticles obtained by a simple co-  
precipitation method

Journal of Applied Research and Technology, vol. 14, núm. 4, 2016, pp. 239-244

Centro de Ciencias Aplicadas y Desarrollo Tecnológico  
Distrito Federal, México

Available in: <http://www.redalyc.org/articulo.oa?id=47447023004>

- How to cite
- Complete issue
- More information about this article
- Journal's homepage in [redalyc.org](http://www.redalyc.org)

[redalyc.org](http://www.redalyc.org)

Scientific Information System

Network of Scientific Journals from Latin America, the Caribbean, Spain and Portugal

Non-profit academic project, developed under the open access initiative



Original

# Heating ability and hemolysis test of magnetite nanoparticles obtained by a simple co-precipitation method

B.I. Macías-Martínez<sup>a</sup>, D.A. Cortés-Hernández<sup>b</sup>, A. Zugasti-Cruz<sup>a</sup>, B.R. Cruz-Ortíz<sup>a</sup>,  
E.M. Múzquiz-Ramos<sup>a,\*</sup>

<sup>a</sup> Facultad de Ciencias Químicas, Universidad Autónoma de Coahuila, Blvd. V. Carranza y José Cárdenas Valdés, C.P. 25280 Saltillo, Coah., México

<sup>b</sup> CINVESTAV IPN-Unidad Saltillo, Industria Metalúrgica 1062, Parque Industrial Saltillo Ramos Arizpe, C.P. 25900 Ramos Arizpe, Coah., México

Received 23 January 2016; accepted 27 May 2016

Available online 2 July 2016

## Abstract

The present paper reports the heating ability and hemolysis test of magnetite nanoparticles (MNPs) for biomedical applications, obtained by a novel and easy co-precipitation method, in which it is not necessary the use of controlled atmospheres and high stirring rates. Different molar proportions of  $\text{FeCl}_2\text{:FeCl}_3$  (2:1 and 3:2 respectively) were used and the obtained MNPs were analyzed by X-ray diffraction, vibrating sample magnetometry and transmission electron microscopy. The heating ability was evaluated under a magnetic field using a solid state induction heating equipment at two different frequencies (362 and 200 kHz). Additionally, a hemolysis test was performed according to the ASTM method. The obtained ferrites showed a particle size in the range of 8–12 nm and superparamagnetic behavior. The MNPs increased the temperature up to 43.1 °C in 5 min under a low magnetic field and showed non hemolytic effect up to 3 mg/ml. The MNPs obtained are highly potential materials for hyperthermia cancer treatment.

All Rights Reserved © 2016 Universidad Nacional Autónoma de México, Centro de Ciencias Aplicadas y Desarrollo Tecnológico. This is an open access item distributed under the Creative Commons CC License BY-NC-ND 4.0.

**Keywords:** Hemolysis test; Heating ability; Nanoparticles

## 1. Introduction

Magnetic particles ranging in size from nanometers to micrometers are attractive materials not only in the field of magnetic recording, but also in the areas of biological and medical applications (Iida, Takayanagi, Nakanishi, & Osaka, 2007). Magnetite nanoparticles (MNPs) are the most studied materials because of their response to magnetic fields through the superparamagnetic behavior at room temperature with high saturation magnetization. In addition, their non-toxicity and high biocompatibility are also suitable for biotechnology areas (Kumar, Inbaraj, & Chen, 2010).

In oncology, hyperthermia is considered to be an artificial way of increasing the body tissue temperature by delivering heat to destroy cancerous cells or prevent their further growth.

The temperature in tumor tissues rises much easier than that in normal tissues, this behavior happens because the tumor tissues have higher heat sensitivity and smaller cooling effect than the normal tissue because of their blood flow (Chicheł, Skowronek, Kubaszewska, & Kanikowski, 2007; Kim et al., 2005b). During hyperthermia treatment, cells undergo heat stress in the temperature range of 41–46 °C resulting in activation and/or initiation of many intra and extracellular degradation mechanisms like protein denaturation, protein folding, aggregation and DNA cross linking. When temperature is increased above 50 °C, necrosis occurs and this treatment is known as thermoablation (Kim et al., 2005a; Kumar & Mohammad, 2011).

Hyperthermia can be induced using magnetic nanoparticles, in a treatment known as magnetic hyperthermia. The nanoparticles can be introduced in the human body in the region surrounding the cancer tumor and then heated up by using an external magnetic field. The dimensions of the nanoparticles used in the hyperthermia method must be less than 100 nm (Doaga et al., 2013).

\* Corresponding author.

E-mail address: [emuzquiz@uadec.edu.mx](mailto:emuzquiz@uadec.edu.mx) (E.M. Múzquiz-Ramos).

Peer Review under the responsibility of Universidad Nacional Autónoma de México.

Iron oxide particles represented by magnetite ( $\text{Fe}_3\text{O}_4$ ) and maghemite ( $\gamma\text{-Fe}_2\text{O}_3$ ) are considered promising candidates for magnetic hyperthermia, because they present biocompatibility, high saturation magnetization, stable magnetic response, higher resistance to oxidation than other metal compounds and relative easiness to functionalize with polymers or functional groups, which makes them excellent candidates for biomedical applications in *in vivo* experiments (Araújo-Neto et al., 2014; Bañobre-López, Teijeiro, & Rivas, 2013).

The biocompatibility of these magnetic nanoparticles is a crucial step for hyperthermia applications; therefore, for any material to be applied for biotechnological usage, it should pass through a strict regimen of various *in vitro* tests, which qualify the material as “compatible”. In other words, when kept in cell culture environment (*in vitro*), it should not lead to detrimental reactions which change the intrinsic properties (cell growth rate, cell morphology, accumulation of unwanted proteins, over-expression of housekeeping and other genes in different tissues, denaturation of structural and functional proteins, among others) of the nearby and distant environment over a period of time. These assessments are done with the help of hemolysis testing, the most common method to determine the hemocompatibility properties of biomaterials (Bahadur & Giri, 2003).

Nanoferrites with a cubic inverse spinel crystalline structure are the appropriate materials for these biomedical applications, in this lattice more octahedral than tetrahedral sites are available and, since these both sites have magnetic moments aligned in opposite directions, a higher magnetization is exhibited. Thus, diverse synthesis methods have been reported to obtain this kind of ferrites, such as sol–gel, co-precipitation, mechanosynthesis, combustion and hydrothermal (Jasso-Terán, Cortés-Hernández, Múzquiz-Ramos, & Sánchez-Fuentes, 2014).

Co-precipitation is a facile and convenient way to synthesize magnetic nanoparticles from aqueous salt solutions, not only is a simple method of synthesis but also has low environmental impact, because it is carried out in aqueous solutions without the use of organic solvents and in conditions of relatively low reaction temperatures (Faraji, Yamini, & Rezaee, 2010). This is done by the addition of a base under inert atmosphere at room temperature or at an elevated temperature. Iron oxide nanoparticles (either  $\text{Fe}_3\text{O}_4$  or  $\gamma\text{-Fe}_2\text{O}_3$ ) and ferrites are usually prepared in an aqueous medium which chemical reaction of formation may be written as Eq. (1).



where M can be  $\text{Fe}^{2+}$ ,  $\text{Mn}^{2+}$ ,  $\text{Co}^{2+}$ ,  $\text{Cu}^{2+}$ ,  $\text{Mg}^{2+}$ ,  $\text{Zn}^{2+}$  or  $\text{Ni}^{2+}$ . Complete precipitation should be expected at pH levels between 8 and 14, with a stoichiometric ratio of 2:1 ( $\text{Fe}^{3+}/\text{M}^{2+}$ ) in a non-oxidizing environment. The size, shape, and composition of the MNPs very much depend on the type of salts used (e.g., chlorides, sulfates, or nitrates), the  $\text{M}^{2+}/\text{Fe}^{3+}$  ratio, the reaction temperature, the pH value, the type of base, the mixing rate, the ionic strength of the media, the reactants addition sequence, and the bubbling of nitrogen gas (Faraji et al., 2010).

Too many studies have been reported (Aldama et al., 2009; Ayala-Valenzuela et al., 2005; Chen et al., 2012; Fabbiyola et al.,

2016; Gordani, Ghasemi, & Saidi, 2014; Kant Sharma & Ghose, 2015; Petcharoen & Sirivat, 2012; Shen et al., 2014; Wu et al., 2007), in all of them high stirring speeds, controlled atmospheres, reaction medium and drying temperatures are used. In this study we propose a very easy method for which the use of controlled atmospheres and high stirring speed is not necessary. We only use mild magnetic stirring, the reactions are carried out in an alkaline atmosphere created by the ammonia solution and the nanoparticles obtained are air dried.

The aim of this work was to synthesize biocompatible MNPs using a novel and easy co-precipitation method in which the use of controlled atmospheres and high stirring rates is not necessary, two different molar proportion  $\text{FeCl}_2:\text{FeCl}_3$  2:1 and 3:2 were tested. Considering the interest in potential biomedical application of MNPs, in particular as a hyperthermia agent for cancer treatment, the heating ability under a magnetic field was carried out in two different frequencies (362 and 200 kHz) and additionally a hemolysis test was performed.

## 2. Materials and methods

### 2.1. Magnetite nanoparticle synthesis

MNPs were prepared using a modified chemical co-precipitation method. Two solutions with different molar ratio of ferric chloride ( $\text{FeCl}_3 \cdot 6\text{H}_2\text{O}$ , Sigma–Aldrich):ferrous chloride ( $\text{FeCl}_2 \cdot 4\text{H}_2\text{O}$ , Sigma–Aldrich) 2:1 and 3:2 were prepared. Each salt was mixed with 25 ml of distilled water into a glass beaker in the required amount to provide molar ratios 2:1 and 3:2. Simultaneously, distilled water was heated up to 70 °C and, under magnetic stirring, concentrated ammonium hydroxide ( $\text{NH}_4\text{OH}$ , Sigma–Aldrich) was added at a required amount to obtain a 1.6 molar aqueous solution allowing enough time for the solution to stabilize at 70 °C. Then, the chloride solution was added dropwise to the ammonia solution until obtaining a black precipitate, corresponding to magnetite, keeping the stirring for 30 min. The precipitate was washed several times with distilled water to remove residual chlorides. The MNPs were air-dried at room temperature.

### 2.2. Characterization of magnetite nanoparticles

The obtained MNPs were analyzed by X-ray diffraction (XRD, Philips 3040) for the crystallographic structure identification and the crystallite size evaluation. The average crystallite size of samples was determined from the full-width at half-maximum (FWHM) of the strongest reflection, using the Scherrer equation. The morphology and grain size were determined by Transmission Electron Microscopy (TEM) (Titan 80300Kv). The magnetic properties of the samples were measured with a SQUID Quantum Design Magnetometer (VSM) in applied fields from –20 to 20 kOe.

### 2.3. Heating capacity

In order to determine if the MNPs have the ability to generate heat, certain quantities of MNPs were placed in a vial with

distilled water. Each vial was stirred in a vortex and then placed in a magnetic induction in a solid state heating equipment (Ambrell, Easy Heat, 0224). The heating capacity of MNPs was measured under two different magnetic field strengths ( $10.2 \text{ kA m}^{-1}$ ; frequency of 362 and 200 kHz), and the quantities of ferrite tested were 7, 9, 11, 13 and 15 mg suspended in 2 ml of distilled water. The resolution of the temperature sensor is  $\pm 0.1^\circ\text{C}$ .

#### 2.4. Hemolysis test

When the external membrane of the erythrocytes is destroyed, hemoglobin is released. It is possible to estimate the amount of destroyed erythrocytes in a given test by measuring the quantity of hemoglobin in a sample. This works as a reference to know the toxicity grade of a dispositive that will be in contact with human blood. The hemolytic activity of the nanoparticles was determined according to a previously reported method (Múzquiz-Ramos, Guerrero-Chávez, Macías-Martínez, López-Badillo, & García-Cerda, 2014).

Human blood was obtained from healthy donors, collected in heparinized-tubes and centrifuged at 3000 rpm for 4 min. The plasma was decanted, the erythrocytes were washed with Alsever's solution (dextrose 0.116 M, sodium chloride 0.071 M, sodium citrate 0.027 M and citric acid 0.002 M at pH 6.4) three times.

The erythrocytes solution was prepared with 100  $\mu\text{l}$  of purified erythrocytes diluted 1:99 with Alsever's solution. A quantity of 150  $\mu\text{l}$  of this solution was added to each individual tube with MNPs (0.25, 0.50 and 3.0 mg/ml). The Alsever's solution and deionized water were used as negative (0% hemolysis) and positive (100% hemolysis) controls, respectively. The tubes were gently mixed using a rotator shaker and then incubated at  $37 \pm 1^\circ\text{C}$  within a shaking water bath for 30 min. Finally, the tubes were centrifuged to measure the hemoglobin by UV–vis light spectrophotometry at a wavelength of 415 nm (Spectronic, model Genesis 5). These tests were performed in triplicate.

### 3. Results and discussions

#### 3.1. Structural properties

Figure 1 shows the XRD patterns of MNPs obtained at two different molar ratios. The crystalline phase identified was magnetite. The main reflections at  $30.1$ ,  $35.4$ ,  $42.9$ ,  $57.5$  and  $62.7$  ( $2\theta$  degrees), for (220), (311), (400), (511) and (440) Miller indexes, respectively (JCPDS card No. 19-0629).

Furthermore, the crystallite sizes ( $D$ ) of the MNPs for the most intense peak (311) plane were calculated from the XRD data based on the Debye-Scherrer formula (Culity, 2001). The crystallite size rises from below to 12.5 nm for the two molar proportions.

#### 3.2. Magnetic properties

The magnetic hysteresis loops of the obtained MNPs are presented in Figure 2. As observed, the magnetic behavior was

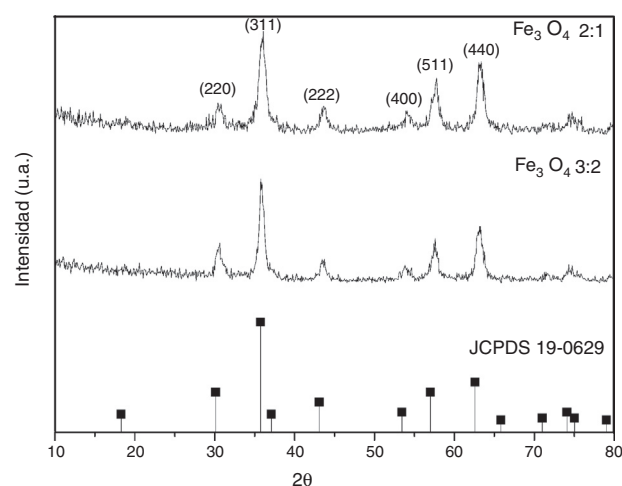


Fig. 1. XRD patterns of MNPs obtained at two different molar proportions of ferric chloride ( $\text{FeCl}_3$ ) and ferrous chloride ( $\text{FeCl}_2$ ) 2:1 and 3:2.

similar in both cases: low coercivity and high magnetic permeability.

The obtained MNPs exhibit superparamagnetic behavior at room temperature, this phenomenon is due to their nanometric size and surface effects which dominate the behavior of the individual magnetic nanoparticles. Frenkel and Dorfman (1930) predicted that a particle of a ferromagnetic material, below a critical particle size ( $<15 \text{ nm}$  for common materials), consists of a single magnetic domain, that is, a particle is in a state of uniform magnetization in any field. In superparamagnetic particles, thermal fluctuations are strong enough to spontaneously demagnetize a previously saturated assembly; therefore, these particles have no hysteresis. Nanoparticles become magnetic in the presence of an external magnet, but they revert to a non-magnetic state when the external magnet is removed. This prevents an 'active' behavior of the particles from happening when there is no applied field. Once introduced in the living systems, particles are 'magnetic' only under the presence of an external field, which gives them a unique advantage when working in biological environments (Frenkel & Dorfman, 1930).

#### 3.3. Transmission electron microscope (TEM) studies

The size and morphology of the synthesized MNPs were performed by the TEM images shown in Figure 3. The results indicated that the nanoparticles are approximately spherical and the mean size is ranged between 8 and 12 nm (Fig. 3a and c), which is consistent with the results obtained by XRD. These sizes are within the allowed range for magnetic hyperthermia applications (Veisich, Gunn, & Zhang, 2010). Figure 3b and d shows the HRTEM micrograph, the corresponding electron-diffraction pattern indicates that the magnetite has a spinel-type structure. Furthermore, the interplanar distances observed  $d = 0.148$ ,  $0.253$ , and  $0.2967 \text{ nm}$  correspond to the crystallographic planes (440), (311) and (220) respectively, which is in line with standard JCPDS card No. 19-0629.



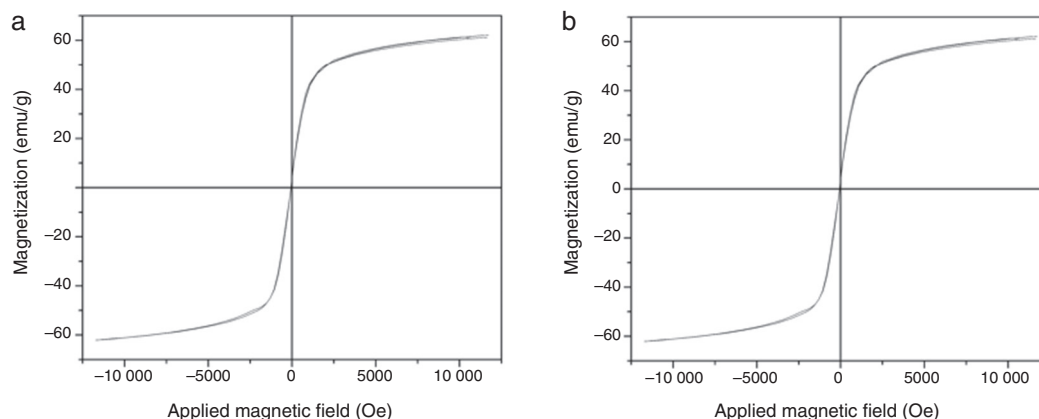


Fig. 2. Hysteresis loops of MNPs obtained at molar ratios 2:1 (a) and 3:2 (b).

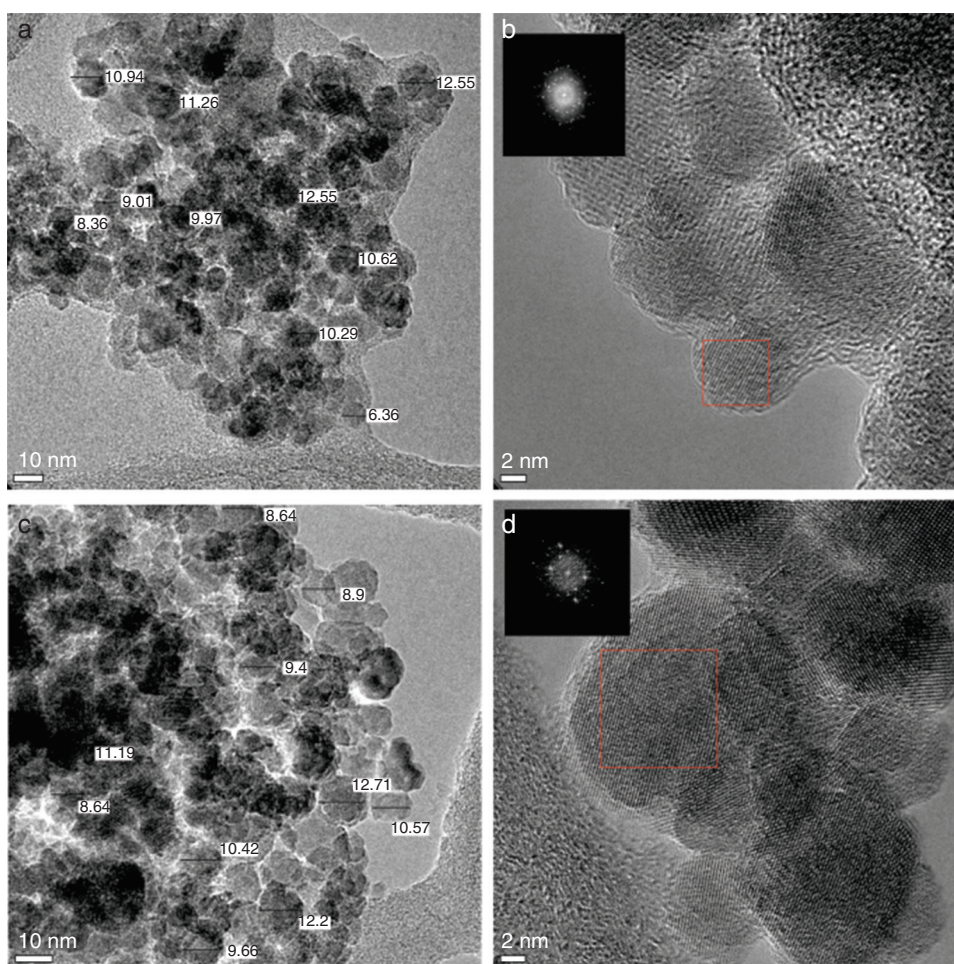


Fig. 3. TEM images of MNPs obtained at molar ratios 2:1 (a) and 3:2 (c), and HRTEM micrograph of magnetite obtained at molar ratios 2:1 (b) and 3:2 (d).

### 3.4. Heating capacity

An important factor that must be considered is the heating ability of the MNPs when a magnetic field is applied; this according to the fact that magnetic hyperthermia consists of raising the temperature in the body through magnetic nanoparticles. When a magnetic nanoparticles system is subjected to an oscillating magnetic field, the absorbed energy is then converted into heat

by several physical mechanisms (Neel relaxations and Brown rotation), and the transformation efficiency strongly depends on the frequency of the external field as well as the nature of the particles such as particle size and surface modification (Ma et al., 2004). The heating capacity of the magnetite nanoparticles was evaluated under an applied magnetic field of  $10.2 \text{ kA m}^{-1}$  and frequencies of 200 kHz (Fig. 4a) and 362 kHz (Fig. 4b). Heating curves of the magnetite obtained at molar ratio 2:1 are

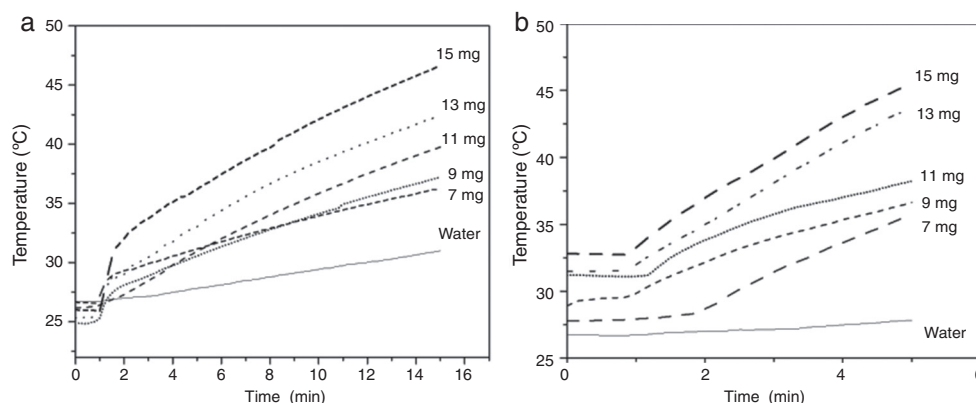


Fig. 4. Magnetic heating of MNPs (7, 9, 11, 13 and 15 mg) suspended in 2 ml of distilled water at  $\nu \sim 362$  kHz and  $H_{max} \sim 10.2$  kA m $^{-1}$  (a) and at  $\nu \sim 200$  kHz and  $H_{max} \sim 10.2$  kA m $^{-1}$  (b).

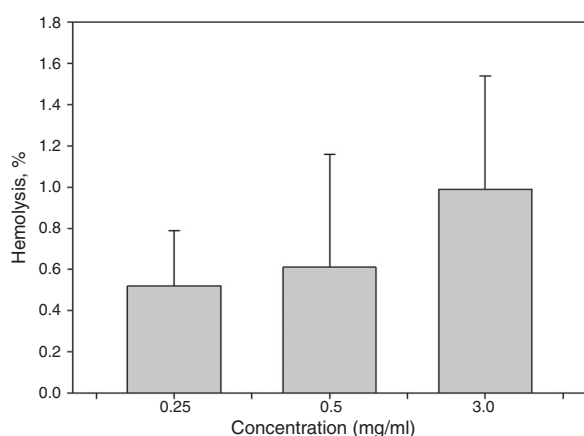


Fig. 5. Hemolysis (%) caused by different MNPs concentrations.

shown in Figure 4, testing 7, 9, 11, 13 and 15 mg of magnetite nanoparticles in 2 ml of distilled water.

As expected, a more rapid increase in temperature is observed when higher concentrations of MNPs are used. Figure 4a shows that the suspension of 13 mg/2 ml reaches temperatures up to 41 °C, in 15 min. When a higher frequency is used (362 kHz) at the same concentration, the 41 °C was reached in just five minutes (Fig. 4b). The obtained temperature for the suspensions at the mentioned concentrations in both frequencies is suitable for magnetic hyperthermia treatment. It is important to highlight the feasibility of selecting between two different treatments: a fast one and a slower one, which may cause less health risk since it has a lower magnetic field.

### 3.5. Hemolysis test

Since these materials are most commonly used in biomedical applications, it is necessary to assess the biocompatibility of the synthesized samples. Thus, a hemolysis assay was conducted. The results of the hemolytic tests (Fig. 5) demonstrated that the hemolysis rates (HRs) of the samples were lower than 2%. These results indicate that the MNPs had non-hemolytic reaction at all tested suspension concentrations up to 3.0 mg/ml. According to

ASTM F 756-08 (ASTMF-756, 2009), HR < 2% produced by any material could be considered as non-hemolytic.

## 4. Conclusions

Using a novel and easy co-precipitation method and molar proportions of FeCl $_2$ :FeCl $_3$  of 2:1 and 3:2, magnetite nanoparticles with a crystallite size between 8 and 12 nm and with spinel structure were obtained. The MNPs exhibit a superparamagnetic behavior, coercivities near to zero and low remanent magnetization. No difference was found in the studied stoichiometric proportions. MNPs showed appropriate heating capacity when they were subjected to an alternating magnetic field of 200 kHz reaching temperatures up to 41 °C in 15 min, while a higher frequency was employed (362 kHz) using the solution at the same concentration, 41 °C was reached in only 5 min. Moreover, these materials showed non-hemolytic activity up to 3 mg/ml.

The results of this work showed that the MNPs are potential materials for magnetic hyperthermia therapy.

## Conflict of interest

The authors have no conflicts of interest to declare.

## Acknowledgments

B.I. Macías thanks CONACyT-México for the financial support (scholarship-102782). This project received financial support from PRODEP México (UACOH-EXB-105).

## References

- Aldama, I., Arévalo, P., Cubero, Á., Pérez, M., Castelaín, M., Antonio, J., et al. (2009). Preparación y estudio de materiales nanoparticulados de óxido de hierro. *Serie Química de Materiales*, 1(4), 15–25.
- Araújo-Neto, R. P., Silva-Freitas, E. L., Carvalho, J. F., Pontes, T. R. F., Silva, K. L., Damasceno, I. H. M., et al. (2014). Monodisperse sodium oleate coated magnetite high susceptibility nanoparticles for hyperthermia applications. *Journal of Magnetism and Magnetic Materials*, 364, 72–79. <http://dx.doi.org/10.1016/j.jmmm.2014.04.001>
- ASTMF-756. (2009). *Standard practice for assessment of hemolytic properties of materials*, Annual Book of ASTM Standards. Committee F04 Medical and

- Surgical Materials and Devices, Subcommittee F04.16 Biocompatibility Test Methods. Annual Book of ASTM Standards.*
- Ayala-Valenzuela, O., Matutes-Aquino, J., Betancourt-Galindo, R., García-Cerda, L., Fernández, O. R., Fannin, P. C., et al. (2005). Magnetite-cobalt ferrite nanoparticles for kerosene-based magnetic fluids. *Journal of Magnetism and Magnetic Materials*, 294, 37–41. <http://dx.doi.org/10.1016/j.jmmm.2005.03.050>
- Bahadur, D., & Giri, J. (2003). Biomaterials and magnetism. *Sadhana*, 28(3), 639–656.
- Bañobre-López, M., Teijeiro, A., & Rivas, J. (2013). Magnetic nanoparticle-based hyperthermia for cancer treatment. *Reports of Practical Oncology & Radiotherapy*, 18(6), 397–400. <http://dx.doi.org/10.1016/j.rpor.2013.09.011>
- Chen, D., Tang, Q., Li, X., Zhou, X., Zang, J., Xue, W., et al. (2012). Biocompatibility of magnetic Fe<sub>3</sub>O<sub>4</sub> nanoparticles and their cytotoxic effect on MCF-7 cells. *International Journal of Nanomedicine*, 7, 4973–4982. <http://dx.doi.org/10.2147/IJN.S35140>
- Chichel, A., Skowronek, J., Kubaszewska, M., & Kanikowski, M. (2007). Hyperthermia – Description of a method and a review of clinical applications. *Reports of Practical Oncology & Radiotherapy*, 12(5), 267–275. [http://dx.doi.org/10.1016/S1507-1367\(10\)60065-X](http://dx.doi.org/10.1016/S1507-1367(10)60065-X)
- Culity, B. D. (2001). *Elements of X-ray diffraction*. New Jersey: Prentice Hall.
- Doaga, A., Cojocariu, A. M., Amin, W., Heib, F., Bender, P., Hempelmann, R., et al. (2013). Synthesis and characterizations of manganese ferrites for hyperthermia applications. *Materials Chemistry and Physics*, 143(1), 305–310. <http://dx.doi.org/10.1016/j.matchemphys.2013.08.066>
- Fabbiyola, S., Kennedy, L. J., Ratnaji, T., Vijaya, J. J., Aruldoss, U., & Bououdina, M. (2016). Effect of Fe-doping on the structural, optical and magnetic properties of ZnO nanostructures synthesised by co-precipitation method. *Ceramics International*, 42(1), 1588–1596. <http://dx.doi.org/10.1016/j.ceramint.2015.09.110>
- Faraji, M., Yamini, Y., & Rezaee, M. (2010). Magnetic nanoparticles: Synthesis, stabilization, functionalization, characterization, and applications. *Journal of the Iranian Chemical Society*, 7(1), 1–37. <http://dx.doi.org/10.1007/BF03245856>
- Frenkel, J., & Dorfman, J. (1930). Spontaneous and induced magnetisation in ferromagnetic bodies. *Nature*, 126, 274–275. <http://dx.doi.org/10.1038/126274a0>
- Gordani, G. R., Ghasemi, A., & Saidi, A. (2014). Enhanced magnetic properties of substituted Sr-hexaferrite nanoparticles synthesized by co-precipitation method. *Ceramics International*, 40(3), 4945–4952. <http://dx.doi.org/10.1016/j.ceramint.2013.10.096>
- Iida, H., Takayanagi, K., Nakanishi, T., & Osaka, T. (2007). Synthesis of Fe<sub>3</sub>O<sub>4</sub> nanoparticles with various sizes and magnetic properties by controlled hydrolysis. *Journal of Colloid and Interface Science*, 314(1), 274–280. <http://dx.doi.org/10.1016/j.jcis.2007.05.047>
- Jasso-Terán, R. A., Cortés-Hernández, D. A., Múzquiz-Ramos, E. M., & Sánchez-Fuentes, H. J. (2014). Synthesis and characterization of zinc and calcium nanoferrites. *Journal of Materials Science: Materials in Medicine*, 25(10), 2221–2228. <http://dx.doi.org/10.1007/s10856-014-5180-x>
- Kant Sharma, R., & Ghose, R. (2015). Synthesis and characterization of nanocrystalline zinc ferrite spinel powders by homogeneous precipitation method. *Ceramics International*, 41(10), 14684–14691. <http://dx.doi.org/10.1016/j.ceramint.2015.07.191>
- Kim, D. H., Lee, S. H., Kim, K. N., Kim, K. M., Shim, I. B., & Lee, Y. K. (2005a). Cytotoxicity of ferrite particles by MTT and agar diffusion methods for hyperthermic application. *Journal of Magnetism and Magnetic Materials*, 293(1), 287–292. <http://dx.doi.org/10.1016/j.jmmm.2005.02.078>
- Kim, D. H., Lee, S. H., Kim, K. N., Kim, K. M., Shim, I. B., & Lee, Y. K. (2005b). Temperature change of various ferrite particles with alternating magnetic field for hyperthermic application. *Journal of Magnetism and Magnetic Materials*, 293(1), 320–327. <http://dx.doi.org/10.1016/j.jmmm.2005.02.077>
- Kumar, C. S. S. R., & Mohammad, F. (2011). Magnetic nanomaterials for hyperthermia-based therapy and controlled drug delivery. *Advanced Drug Delivery Reviews*, 63(9), 789–808. <http://dx.doi.org/10.1016/j.addr.2011.03.008>
- Kumar, R., Inbaraj, B. S., & Chen, B. H. (2010). Surface modification of superparamagnetic iron nanoparticles with calcium salt of poly(-glutamic acid) as coating material. *Materials Research Bulletin*, 45(11), 1603–1607. <http://dx.doi.org/10.1016/j.materresbull.2010.07.017>
- Ma, M., Wu, Y., Zhou, J., Sun, Y., Zhang, Y., & Gu, N. (2004). Size dependence of specific power absorption of Fe<sub>3</sub>O<sub>4</sub> particles in AC magnetic field. *Journal of Magnetism and Magnetic Materials*, 268(1–2), 33–39. [http://dx.doi.org/10.1016/S0304-8853\(03\)00426-8](http://dx.doi.org/10.1016/S0304-8853(03)00426-8)
- Múzquiz-Ramos, E. M., Guerrero-Chávez, V., Macías-Martínez, B. I., López-Badillo, C. M., & García-Cerda, L. A. (2014). Synthesis and characterization of maghemite nanoparticles for hyperthermia applications. *Ceramics International*, 41(1), 397–402. <http://dx.doi.org/10.1016/j.ceramint.2014.08.083>
- Petcharoen, K., & Sirivat, A. (2012). Synthesis and characterization of magnetite nanoparticles via the chemical co-precipitation method. *Materials Science and Engineering: B*, 177(5), 421–427. <http://dx.doi.org/10.1016/j.mseb.2012.01.003>
- Shen, L., Qiao, Y., Guo, Y., Meng, S., Yang, G., Wu, M., et al. (2014). Facile co-precipitation synthesis of shape-controlled magnetite nanoparticles. *Ceramics International*, 40(1), 1519–1524. <http://dx.doi.org/10.1016/j.ceramint.2013.07.037>
- Veisheh, O., Gunn, J. W., & Zhang, M. (2010). Design and fabrication of magnetic nanoparticles for targeted drug delivery and imaging. *Advanced Drug Delivery Reviews*, 62(3), 284–304. <http://dx.doi.org/10.1016/j.addr.2009.11.002>
- Wu, J.-H., Ko, S. P., Liu, H.-L., Kim, S., Ju, J.-S., & Kim, Y. K. (2007). Sub 5 nm magnetite nanoparticles: Synthesis, microstructure, and magnetic properties. *Materials Letters*, 61(14–15), 3124–3129. <http://dx.doi.org/10.1016/j.matlet.2006.11.032>